

NMR study of a magnetic phase transition in $\text{Ca}_3\text{CuNi}_2(\text{PO}_4)_4$: A spin trimer compound

M. Ghosh, K. Ghoshray,* M. Majumder, B. Bandyopadhyay, and A. Ghoshray
ECMP Division, Saha Institute of Nuclear Physics, 1/AF Bidhannagar, Kolkata 700064, India

(Received 14 October 2009; revised manuscript received 16 December 2009; published 12 February 2010)

^{31}P nuclear-magnetic-resonance (NMR) studies have been performed in trimer spin chain compound $\text{Ca}_3\text{CuNi}_2(\text{PO}_4)_4$, in the temperature range 4–300 K. In the range 16–300 K, the spectrum corresponds to a typical overlap of two powder patterns, consistent with two inequivalent phosphorous sites, having different shift parameters. A comparison of the isotropic hyperfine field ($H_{\text{hf}}^{\text{iso}}$) and the axial part ($H_{\text{hf}}^{\text{ax}}$) obtained in the paramagnetic phase of $\text{Ca}_3\text{CuNi}_2(\text{PO}_4)_4$, with those obtained in $\text{Ca}_3\text{Cu}_3(\text{PO}_4)_4$, suggest a stronger interchain exchange interaction in $\text{Ca}_3\text{CuNi}_2(\text{PO}_4)_4$, which is possibly the reason for the higher antiferromagnetic transition temperature in $\text{Ca}_3\text{CuNi}_2(\text{PO}_4)_4$. The temperature dependence of the spin-lattice relaxation rate ($1/T_1$) shows a clear signature of long-range magnetic order in $\text{Ca}_3\text{CuNi}_2(\text{PO}_4)_4$ below 16 K (T_N). T_N agrees quite satisfactorily with that obtained from the derivative of the molar susceptibility versus T plot. The NMR line shape below T_N shows the signature of a considerable distribution of the internal magnetic field in the ordered state with the existence of two magnetic sublattices with opposite direction of polarization with respect to the direction of the external magnetic field. A comparison of the behavior of the $1/T_1$ data in $\text{Ca}_3\text{CuNi}_2(\text{PO}_4)_4$ with those in $\text{Sr}_3\text{Cu}_3(\text{PO}_4)_4$ clearly suggests that the mechanism of the relaxation changes from a two magnon-mediated Raman process in the former to a three magnon-mediated process in the latter.

DOI: [10.1103/PhysRevB.81.064409](https://doi.org/10.1103/PhysRevB.81.064409)

PACS number(s): 75.50.Ee, 75.30.Et, 76.60.-k

I. INTRODUCTION

Low-dimensional quantum spin system is a fascinating subject of interest because it exhibits many unusual as well as interesting physical phenomena due to the dominance of quantum effects.¹ The ground state and low lying excitations depend on the spin value in Heisenberg antiferromagnetic (HAF) uniform chain. While it is a quantum disordered state (spin liquid) and the magnetic excitation is gapless in a spin-1/2 HAF uniform chain, a gap exists in the excitation spectrum for integer spin values.²

A gap also exists in $S=1/2$ HAF bond alternating chains with $0 < \alpha \leq 1$,³ where the alteration parameter $\alpha = J_2/J_1$ and the two exchange interaction parameters, J_2 and J_1 are $J(1 \pm \alpha)$. Recently it has been suggested that $S=1/2$ AF chain with period 3 exchange coupling shows a plateau in the magnetization curve at magnetization per site $m=1/6$ (1/3 of the full magnetization).⁴ This phenomenon in quantum spin chains is analogous to the quantum Hall effect-topological quantization of a physical quantity under a changing magnetic field. A trimer chain is the first spin system that has been predicted to show a magnetization plateau. Examples of spin trimer systems are rare in nature. Few compounds known to date include $\text{La}_4\text{Cu}_3\text{MoO}_{12}$ in which the three Cu^{2+} spins form a triangle so that the AF intratrimer interactions are frustrated,⁵ nevertheless the system undergoes an AF ordering near 2.6 K.

$\text{A}_3\text{Cu}_3(\text{PO}_4)_4$ ($\text{A} \equiv \text{Ca, Sr, Pb}$) is another spin trimer system in which the intertrimer exchange interaction J_2 is 3 K while the intratrimer interaction J_1 is about 126 K.^{6,7} As a result of this the ground state of this compound is a doublet and is a model system of linear HAF trimer. In principle, such a doublet ground state can be changed into a singlet ground state by substituting a Cu^{2+} ($S=1/2$) spin in the trimer by Ni^{2+} ($S=1$). This would offer the opportunity of realizing a gapped quantum spin trimer system. To investigate

this Podlesnyak *et al.*⁸ studied inelastic neutron scattering in $\text{Ca}_3\text{Cu}_{3-x}\text{Ni}_x(\text{PO}_4)_4$ ($x=0, 1, \text{ and } 2$). They have shown that for $x=1$, three types of trimer: Cu2-Cu1-Cu2, Cu2-Cu1-Ni, and Ni-Cu1-Ni are created. As a result the singlet ground state could not be realized in this system. For $x=2$, only trimer of the type Ni-Cu-Ni are present. Moreover for $x=1$, $J_{\text{Cu-Cu}}$ has been found to enhance to -4.92 meV from -4.74 meV observed in $x=0$ and $J_{\text{Cu-Ni}} = -0.85$ meV for $x=1$ and 2. It was further shown from structural investigation using elastic neutron-scattering study that the middle position of a trimer, in each case with $x=1$ and 2, is occupied by the Cu1 atom and the Ni atoms prefer the end positions, which were occupied by Cu2 atoms in the parent compound ($x=0$).⁹ These results along the magnetic-susceptibility measurements further confirm that $x=2$ compound undergoes an AF transition at 20 K (T_N), whereas the $x=1$ compound does not order down to 1.5 K and follows the Curie-Weiss law in the range 1.5–300 K. On the other hand, the pure compound ($x=0$) was reported to undergo a ferromagnetic transition at $T_C=0.91$ K and the χ^{-1} vs T curve shows a clear signature of a reduction in the value of the net spin of a trimer to one third of its value below 45 K.⁷ This strongly suggests the dominance of nearest-neighbor (NN) AF coupling compared to that of the next-nearest-neighbor interaction in the pure compound. Furthermore, it follows from the neutron-scattering results that the replacement of one Cu^{2+} ($S=1/2$) by a Ni^{2+} ($S=1$) reduces appreciably the magnitude of the NN AF interaction within a trimer. As a consequence, the net spin of each trimer remain unchanged down to 1.5 K. Thus the partial replacement of Cu^{2+} by Ni^{2+} in a trimer alters the magnetic property of $\text{Ca}_3\text{Cu}_3(\text{PO}_4)_4$ significantly.

The motivation of the present work is to study the local magnetic properties of $\text{Ca}_3\text{CuNi}_2(\text{PO}_4)_4$ using ^{31}P nuclear-magnetic resonance (NMR). Figure 4 of Ref. 9 shows the trimers when projected in the ab plane in $\text{Ca}_3\text{Cu}_3(\text{PO}_4)_4$. In $\text{Ca}_3\text{CuNi}_2(\text{PO}_4)_4$, the Cu2 positions at the ends of a trimer

would be occupied by Ni ions. It also shows the bonding of the magnetic ions within a trimer, with two types of phosphorous atoms, viz., P1 and P2 present in the unit cell, via the oxygen atoms. From the figure it is seen that P1 atom is bonded with Cu1 and Ni spins in a trimer, therefore it can probe the intratrimer exchange interaction through the transferred hyperfine interaction. P2 connects the Ni spins of the trimer belonging to the neighboring chains and therefore can probe the intertrimer exchange. Thus having only one type of trimer, NMR would provide valuable information on both intratrimer and intertrimer exchange interactions including the electron-spin dynamics.

II. EXPERIMENT

Polycrystalline sample of $\text{Ca}_3\text{CuNi}_2(\text{PO}_4)_4$ was synthesized using solid-state reaction method by heating a stoichiometric mixture of CuO (99.99%), NiO (99.99%), CaCO_3 (99.99%), and $\text{NH}_4\text{H}_2\text{PO}_4$ (99.99%) very slowly up to 600 °C and then annealed at 900 °C during 120 h, with several intermediate grindings. The sample is characterized at room temperature using x-ray diffraction with Cu $K\alpha$ radiation ($\lambda=1.5406$ Å). All the peaks can be indexed on the basis of monoclinic structure with space group $C2/c$ and cell parameters: $a=17.716(1)$ Å, $b=4.820(2)$ Å, $c=17.846(1)$ Å, and $\beta=123.64(1)^\circ$ which agree satisfactorily with the reported values.⁹ The dc magnetic susceptibility was measured in a superconducting quantum interference device magnetometer of Quantum Design (MPMS) in a magnetic field of 0.1 T in the temperature range 4–300 K in the heating cycle. The NMR measurements were carried out in the fields of $H=1.39$ T ($\nu_R=24.005$ MHz) and at $H=7.04$ T ($\nu_R=121.423$ MHz) using a conventional phase-coherent Themway PROT4103 pulse spectrometer. The spectrum was recorded by changing the frequency step by step and recording the spin-echo intensity by applying a $\pi/2-\tau-\pi/2$ solid echo sequence. The temperature variation studies in the range 4–300 K were performed in an Oxford continuous flow cryostat with a ITC503 controller. Shift is measured with respect to the position of the ^{31}P NMR line (ν_R) in H_3PO_4 solution.

III. RESULTS AND DISCUSSION

A. Magnetic-susceptibility measurement

Figure 1 shows the variation in magnetic susceptibility, χ_M with temperature in $\text{Ca}_3\text{CuNi}_2(\text{PO}_4)_4$. The nature of the curve is similar to that reported by Pomjakushin *et al.*⁹ Observation of a comparatively broad peak at the antiferromagnetic transition temperature ($T_N=20$ K) suggests the dominance of one-dimensional nature of magnetism in this trimer spin chain compound. The enhancement of χ in the range 4–10 K was also present in the result reported by the earlier authors. It could arise from some impurity phase present in the sample or from an intrinsic contribution of the compound itself. Above 50 K, χ_M followed well the Curie-Weiss behavior, with the Curie constant $C=2.78$ emu K/mole and Weiss constant $\theta=-26$ K. The paramagnetic spin value per magnetic site $\text{Cu}^{2+}/\text{Ni}^{2+}$ calculated from the value of C ,

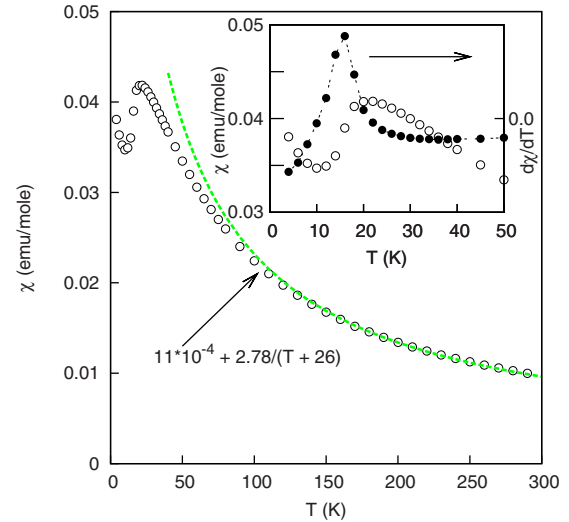


FIG. 1. (Color online) Variation in magnetic susceptibility with temperature in $\text{Ca}_3\text{CuNi}_2(\text{PO}_4)_4$, measured in a field of 0.1 T. Curie-Weiss behavior represented by dashed line. The inset shows the variation in χ and $d\chi/dT$ with T in the range 4–50 K.

amounted to $S_{av}=0.95$. All these values agree well with those reported previously.⁹ The inset of Fig. 1 shows the variation in the derivative of χ with T which shows a sharp fall around 16 K, indicating the actual AF ordering temperature in this compound.

B. NMR spectra and shift parameters

Figure 2 shows the ^{31}P NMR spectra in $\text{Ca}_3\text{CuNi}_2(\text{PO}_4)_4$ at different temperatures in a field of 7 T. At any temperature in the range 26–300 K the spectrum shows a typical overlap of two powder patterns for nuclear spin $I=1/2$, having different component of shift parameters. In the range 16 K $< T < 26$ K the linewidth of the individual components increases appreciably so that the overall spectrum looks like a single broad line. Below 16 K, in addition to this line toward the high-frequency side of ν_R , there appears a new line toward the lower frequency side of ν_R . Intensity of this new line gradually increases till 9 K. Below this temperature, no further enhancement in intensity of this line is observed. Furthermore, the width of the line toward the high-frequency side of ν_R increases appreciably below 16 K, where the bulk susceptibility showed a decreasing trend. Therefore, this enhancement of linewidth gives a microscopic evidence of the development of long range magnetically ordered state below 16 K. The large linewidth also indicates the extent of internal magnetic field distribution in the ordered state. From the present NMR experiment in a field of 7 T, the magnetic ordering temperature appears to be in the range 14.8 K $< T_N < 16$ K, which is very close to that observed from the $d\chi/dT$ vs T plot (inset of Fig. 1). Furthermore, the appearance of a new line on the low-frequency side of ν_R in addition to that at the high-frequency side of ν_R indicates the presence of two sublattices with opposite direction of the electronic spin polarizations with respect to the direction of the external magnetic field.¹⁰ It is to be noted that even in the

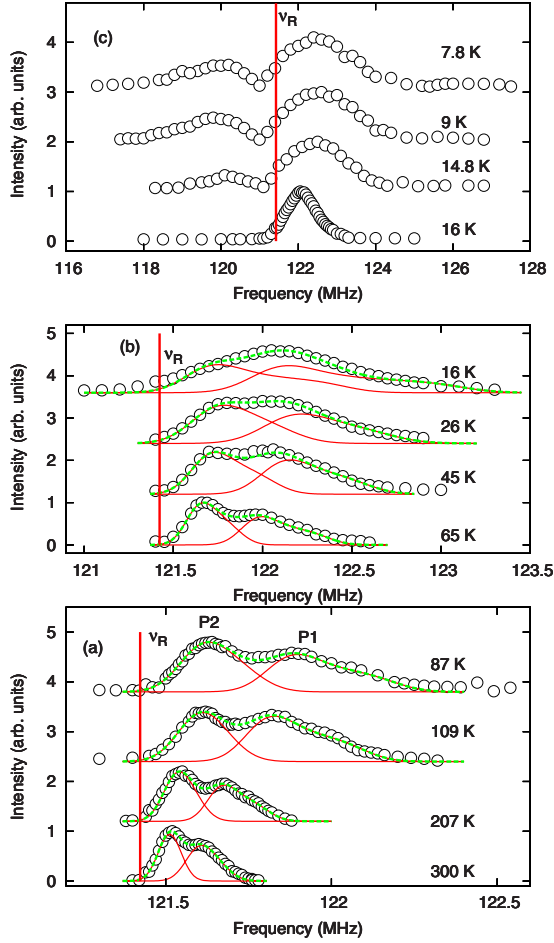


FIG. 2. (Color online) ^{31}P NMR spectra of polycrystalline $\text{Ca}_3\text{CuNi}_2(\text{PO}_4)_4$ at different temperatures recorded at $H=7$ T (represented by open circles). Theoretical line used to fit the experimental spectra (dashed line), along with two constituent lines (continuous lines) corresponding to resonance lines of two inequivalent phosphorous atoms are also shown. Vertical line represents reference position at frequency 121.423 MHz.

ordered state though the linewidth increases appreciably, the line position is not altered significantly with respect to that in the paramagnetic state. This indicates that the local magnetic field (H_{local}) at the ^{31}P site even in the AF ordered state is not much enhanced compared to that in the paramagnetic state. Possible reason for this could be the reduction in the magnitude of H_{local} at the ^{31}P nuclear site due to the nearly antiparallel alignment of the electronic spins of the neighboring ions in the AF ordered state. Over and above a further reduction in H_{local} could also arise from considerable quenching of the Cu^{2+} moments due to the presence of two different sublattices a and b with antiferromagnetic and ferromagnetic intratrimer spin alignments as suggested from neutron scattering.⁹ In order to determine the shift parameters, the experimental spectra in the whole temperature range are fitted to the equation

$$\nu = \nu_R [1 + K_{\text{iso}} + K_{\text{ax}}(3 \cos^2 \theta - 1) + K_{\text{an}} \sin^2 \theta \cos 2\phi],$$

where K_{iso} , K_{ax} , and K_{an} are the isotropic, axial, and the anisotropic parts of the shift, respectively, arising from H_{local}

produced at the ^{31}P nucleus site due to the electron-nuclear hyperfine and the dipolar interaction. ν_R is the reference frequency as mentioned earlier. θ and ϕ are the Euler angles between the principal axes of the hyperfine coupling tensor and the direction of the external magnetic field (Zeeman field).

In the temperature range 16–300 K, the experimental spectra are well fitted by considering the theoretical line as a superposition of two lines with different values of shift parameters, with the internal field being axially symmetric for both the sites as it was in the pure compounds $\text{Ca}_3\text{Cu}_3(\text{PO}_4)_4$ and $\text{Sr}_3\text{Cu}_3(\text{PO}_4)_4$.^{11,12} Thus the substitution of two Cu atoms by Ni atoms does not affect the nature of the anisotropy of the internal field at the ^{31}P sites. These two constituent lines should correspond to two types of phosphorous atoms present in the unit cell of $\text{Ca}_3\text{CuNi}_2(\text{PO}_4)_4$. As the intertrimer exchange interaction is weak compared to the intratrimer exchange interaction, so the spectral line with larger shift is assigned as due to P1, which is bonded with Cu^{2+} and Ni^{2+} ions within a trimer, and that with the smaller shift due to P2, bonded with Ni^{2+} ions of trimer belonging to neighboring chains. Figure 2(a) and 2(b) shows the theoretical spectrum superimposed on the experimental line together with the two constituent lines corresponding to P1 and P2 in the temperature range 16–300 K. Figure 3(a) and 3(b) show the temperature dependence of K_{iso} and K_{ax} , respectively, for P1 and P2. Both the shift parameters increases continuously with decreasing temperature in the range 300–75 K for the two sites. Below 75 K, this is further enhanced particularly for P1 site which could be a signature of the development of short-range magnetic correlation within the trimer chain.

We have also performed the NMR experiment at a much lower resonance frequency of 24 MHz with $H=1.39$ T. In this case below 60 K, the shift parameters could not be determined accurately, because of the poor S/N ratio, due to the line broadening for critical slowing down of the electron-spin fluctuations. However, when the measurements were done in a field of 7 T, with $\nu=121$ MHz, due to the much enhanced signal sensitivity at a higher resonance frequency, the S/N ratio remains satisfactory throughout the range 4–300 K, even in the critical spin fluctuation dominated regime and hence offers the opportunity of recording the spectra close to T_N . The shift parameters obtained by fitting the spectra recorded at $H=1.39$ T in the range 60–300 K are also included in Fig. 3. The close agreement between the values obtained by analyzing the spectra at two widely different resonance frequencies justifies the accuracy of the obtained parameters.

The shift is related to χ_{spin} by the relation

$$K = K_0 + \frac{H_{\text{hf}}}{N\mu_B} \chi_{\text{spin}}(T), \quad (1)$$

where H_{hf} is the hyperfine field, K_0 is the chemical shift, N is the Avogadro number, and $\chi_{\text{spin}}(T)$ is the contribution of electronic spin to the magnetic susceptibility. As long as hyperfine field remains constant, K should follow $\chi(T)$. Contribution to H_{hf} arises from the transferred hyperfine interaction, which is a property of the electronic structure and the dipolar interaction, neither of which is temperature depen-

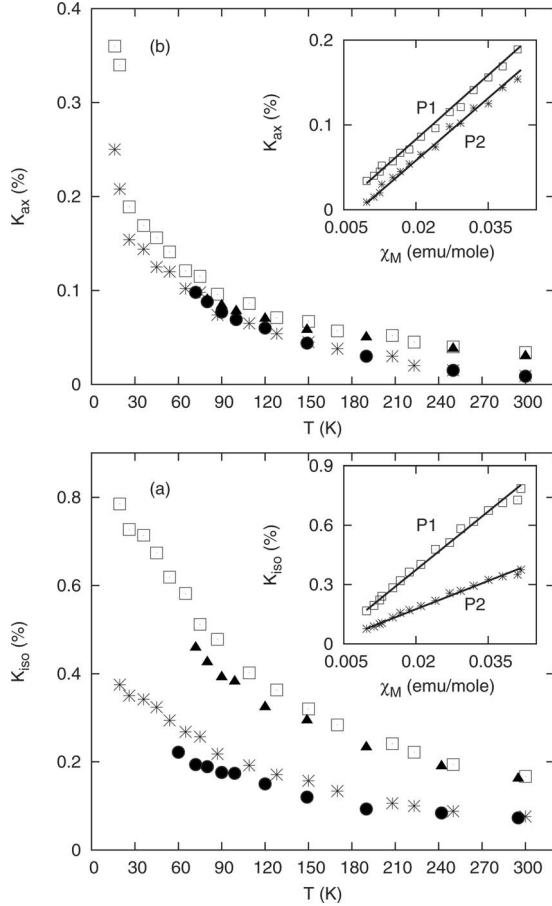


FIG. 3. Temperature variation in (a) K_{iso} and (b) K_{ax} in the temperature range 16–300 K, measured in a field $H=7$ T: open square is for P1 site and star is for P2 site, and in $H=1.39$ T: solid-black triangle is for P1 site and solid-black circle is for P2 site. Inset shows the variation in (a) K_{iso} and (b) K_{ax} for both P1 and P2 sites against χ_M with temperature as implicit parameter.

dent. Although $K(T)$ need not have the same symmetry as $\chi(T)$, the temperature dependence of $K(T)$ should reflect that of $\chi(T)$. The inset of Figs. 3(a) and 3(b) shows that both K_{iso} and K_{ax} varies linearly with $\chi(T)$ in the range 26–300 K. This linearity suggests unique hyperfine coupling constant over this temperature range. By using the above relation we can determine the values of isotropic and the axial parts of the hyperfine field for these two sites. Table I shows the values of H_{hf}^{iso} and H_{hf}^{ax} for the P1 and P2 sites for the compound $\text{Ca}_3\text{CuNi}_2(\text{PO}_4)_4$ together with those obtained in $\text{Ca}_3\text{Cu}_3(\text{PO}_4)_4$ (from our measurement) for comparison.

It is seen that for P2 site (which probes the interchain exchange), both the isotropic and the axial parts of hyperfine fields are enhanced in $\text{Ca}_3\text{CuNi}_2(\text{PO}_4)_4$ compared to that in

$\text{Ca}_3\text{Cu}_3(\text{PO}_4)_4$. As the dipolar field has negligible contribution to H_{hf}^{iso} , therefore an increase in the magnitude of H_{hf}^{iso} , indicates an enhancement of hyperfine contribution which could result from an increase in the interchain exchange interaction. On the other hand H_{hf}^{ax} contains both hyperfine and the dipolar contributions, so its increase should signify an enhancement of both these contributions in $\text{Ca}_3\text{CuNi}_2(\text{PO}_4)_4$. As the dipolar contribution is proportional to the bulk susceptibility and we have used the susceptibility of randomly oriented powder sample for estimating H_{hf}^{ax} from K_{ax} versus $\chi(T)$ plot [inset of Fig. 3(b)], the anisotropies of the shift should be attributed only to the hyperfine contribution. To estimate more exact value of the hyperfine coupling constant, for each direction, it is necessary to measure the anisotropy of the susceptibility by using a single-crystal sample and to analyze the shift data by using the K versus χ plot. Nevertheless, the present findings clarify the reason for the higher magnetic ordering temperature in $\text{Ca}_3\text{CuNi}_2(\text{PO}_4)_4$. On the other hand in case of P1 site, the magnitude of H_{hf}^{iso} in $\text{Ca}_3\text{CuNi}_2(\text{PO}_4)_4$ is seen to be smaller compared to that in $\text{Ca}_3\text{Cu}_3(\text{PO}_4)_4$. This indicates a decrease in the nearest-neighbor intrachain exchange in the former compared to that in the latter, which agrees with the suggestion from neutron scattering.⁹

C. Nuclear-spin-lattice relaxation rates

To gain more insight about the dynamics of the magnetic phase transition in the trimer spin chain compound $\text{Ca}_3\text{CuNi}_2(\text{PO}_4)_4$, which orders at a considerably higher temperature compared to the few such known compounds, we measured the spin-lattice relaxation rate $1/T_1$, which is a very sensitive probe of the low-energy electron-spin fluctuations, as a function of temperature. $1/T_1$ is measured by the saturation recovery method using a single $\pi/2$ pulse. Measurements were performed in presence of the external magnetic fields of 7 and 1.39 T in order to see whether the strong-field dependence of $1/T_1$ reported in case of $\text{Ca}_3\text{Cu}_3(\text{PO}_4)_4$ (Ref. 11) is also present in $\text{Ca}_3\text{CuNi}_2(\text{PO}_4)_4$. We have also measured ^{31}P $1/T_1$ in isostructural $\text{Sr}_3\text{Cu}_3(\text{PO}_4)_4$ at $H=7$ T for which the same at $H=1.39$ T was reported earlier.¹² Figure 4 shows the variation in $1/T_1$ with T for $\text{Ca}_3\text{CuNi}_2(\text{PO}_4)_4$ at $H=7$ T in the range 4–300 K and those measured at $H=1.39$ T in the range 60–300 K, due to the reason discussed in Sec. III B. It is to be mentioned that $1/T_1$ of P1 and P2 sites are not same throughout the whole temperature range for both 1.39 and 7 T. The inset shows the variation in $1/T_1$ with T at two different fields $H=1.39$ and 7 T in $\text{Sr}_3\text{Cu}_3(\text{PO}_4)_4$. In this compound, the values of $1/T_1$ for P1 and P2 sites are same for both fields. It is seen that $1/T_1$ in $\text{Sr}_3\text{Cu}_3(\text{PO}_4)_4$ is strongly field dependent

TABLE I. Values of ^{31}P hyperfine fields.

Compound	H_{hf}^{iso} for P1 (kOe/ μ_B)	H_{hf}^{iso} for P2 (kOe/ μ_B)	H_{hf}^{ax} for P1 (kOe/ μ_B)	H_{hf}^{ax} for P2 (kOe/ μ_B)
$\text{Ca}_3\text{CuNi}_2(\text{PO}_4)_4$	1.103 ± 0.005	0.538 ± 0.009	0.278 ± 0.002	0.273 ± 0.003
$\text{Ca}_3\text{Cu}_3(\text{PO}_4)_4$	1.172 ± 0.007	0.423 ± 0.005	0.279 ± 0.003	0.267 ± 0.005

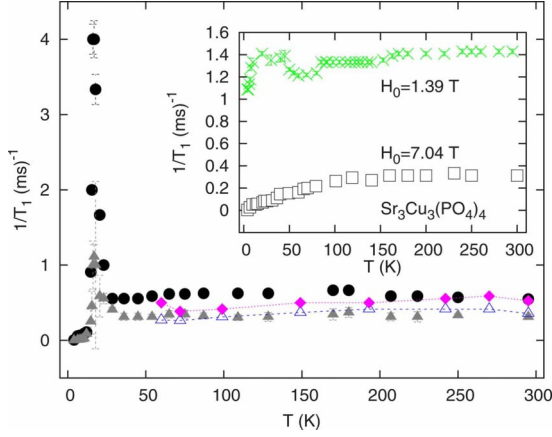


FIG. 4. (Color online) Variation in $1/T_1$ with T in $\text{Ca}_3\text{CuNi}_2(\text{PO}_4)_4$ for two fields: solid-black circle is for P1 and solid-gray triangle is for P2 when $H=7$ T. Solid-square magenta is for P1 and open-blue triangle is for P2 when $H=1.39$ T. Inset shows the $1/T_1$ vs T curves in $\text{Sr}_3\text{Cu}_3(\text{PO}_4)_4$ for $H=1.39$ and 7 T. The error bar in each data corresponds to the size of the symbol.

as reported in case of isostructural $\text{Ca}_3\text{Cu}_3(\text{PO}_4)_4$, whereas the same in $\text{Ca}_3\text{CuNi}_2(\text{PO}_4)_4$ shows negligible field dependence. This shows that the substitution of Ni^{2+} ($S=1$) in place of Cu^{2+} ($S=1/2$) strongly influences the relaxation mechanism. $1/T_1$ in such compounds is governed by the thermal excitations of the $3d$ spins and can be written as

$$\frac{1}{T_1} = 2\gamma_n^2 k_B T \sum |A(\mathbf{q})|^2 \chi''(\mathbf{q}, \omega_n) / \omega_n, \quad (2)$$

where γ_n is the nuclear gyromagnetic ratio, $A(\mathbf{q})$ is the wave-vector-dependent hyperfine coupling, and $\chi''(\mathbf{q}, \omega_n)$ is the dissipative component of the chain dynamic susceptibility evaluated at the nuclear Larmor frequency ω_n .¹³ The values of $1/T_1$ in $\text{Ca}_3\text{CuNi}_2(\text{PO}_4)_4$ remains almost constant with temperature from 300 to 26 K for both the sites. This is a typical feature of fast spin fluctuation ($\omega_e \gg \omega_n$) of the paramagnetic moments. Within the localized spin model in a high-temperature limit,¹³ the value of $1/T_1$ at a nonmagnetic nucleus can be written as

$$\frac{1}{T_1} = \sqrt{2\pi} (2\gamma_n H_{hf})^2 z' S(S+1) / (3\omega_{ex}) \quad (3)$$

with the exchange frequency of local spins $\omega_{ex} = k_B |\theta_{cw}| / [\hbar \sqrt{zS(S+1)/6}]$. The constants $z=2$ and $z'=2$ correspond to the numbers of exchange-coupled local spins and those of the local spins interacting with the probing nucleus, respectively.¹⁴ Taking $\gamma_n = 1.083 \times 10^8 \text{ s}^{-1} \text{ T}^{-1}$ for the phosphorous nucleus, $H_{hf}^{iso} \approx 1.103 \text{ kOe} / \mu_B$ for P1 and $H_{hf}^{iso} \approx 0.538 \text{ kOe} / \mu_B$ for P2, $\theta = -26 \text{ K}$, and $S=1$ for the spin of Ni^{2+} and $S=1/2$ for Cu^{2+} , the theoretical value of T_1 is 3.19 ms for P1 and 9.24 ms for P2. These calculated values are approximately three times greater than the experimental values of $T_1 = 1.82 \text{ ms}$ for P1 and $T_1 = 3.2 \text{ ms}$ for P2. The discrepancy suggests some additional mechanism such as the orbital fluctuations may contribute to the spin-lattice relaxation process in the paramagnetic state of $\text{Ca}_3\text{CuNi}_2(\text{PO}_4)_4$.

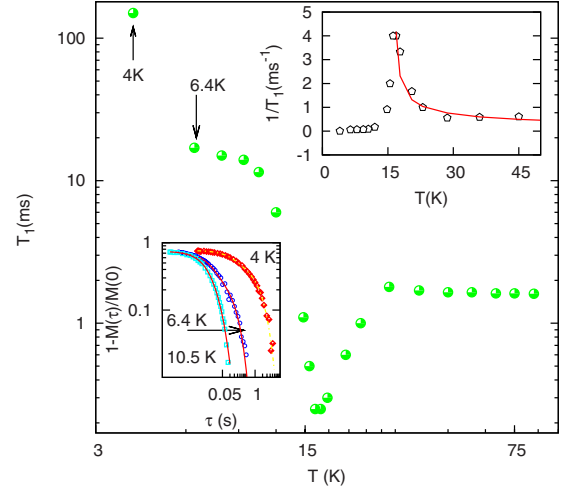


FIG. 5. (Color online) Temperature variation in $1/T_1$ for P1 site in $\text{Ca}_3\text{CuNi}_2(\text{PO}_4)_4$ in the range 4–100 K. Upper inset shows a critical behavior $\frac{1}{T_1} \propto \left[\frac{T-T_N}{T_N}\right]^{-\alpha}$ near magnetic ordering temperature 16 K with $\alpha=0.5$ for P1 site. Lower inset shows the spin-lattice relaxation decay curve for 4, 6.4, and 10.5 K.

Below 26 K, $1/T_1$ starts to enhance indicating the effect of the slowing down of the $3d$ spin fluctuations below this temperature. Appearance of a pronounced peak at 16 K clearly suggests the occurrence of a magnetic phase transition at this temperature. In the range 6.4–16 K, $1/T_1$ decreases sharply indicating a pronounced reduction in the contribution of $3d$ spin fluctuations to ^{31}P nuclear relaxation process. Interestingly, the value of T_1 is enhanced by an order of magnitude with in the temperature interval of 4–6.4 K, as seen from Fig. 5. This is further clarified from the decay curves at 10.5, 6.4, and 4 K shown in the lower inset of Fig. 5. This finding could be a signature of another phase transition occurring at further lower temperature below 4 K. To study this in detail, measurement of $1/T_1$ well below 4 K is necessary, which could not be performed because of our experimental limitations. The strong-field dependence of ^{31}P $1/T_1$ reported in case of $\text{Ca}_3\text{Cu}_3(\text{PO}_4)_4$ was explained satisfactorily by the exchange enhanced three magnon-mediated relaxation process suggested theoretically.¹¹ Similar behavior of $1/T_1$ in $\text{Sr}_3\text{Cu}_3(\text{PO}_4)_4$, observed from the present measurements (inset of Fig. 4) further confirms that the relaxation mechanism remains same for substitution of Ca by Sr. However, replacement of Cu by Ni almost suppresses the influence of magnetic field on $1/T_1$ process. This finding suggests a negligible contribution of three magnon scattering process to $1/T_1$ of $\text{Ca}_3\text{CuNi}_2(\text{PO}_4)_4$. The dominant contribution arises from two magnon-mediated Raman processes due to exchange scattering,¹³ which is expected to be field independent. In order to check this finding with the theoretical prediction of Hori and Yamamoto¹⁵ we have calculated values of $k_B T / J_{\text{Cu-Ni}} = 1.01$ with $J_{\text{Cu-Ni}} = -0.85 \text{ meV}$ and $T = 10 \text{ K}$ together with those of $\hbar \gamma_n H / J = 1 \times 10^{-4}$ and 5×10^{-4} , respectively, with $H = 1.39$ and 7 T for $\text{Ca}_3\text{CuNi}_2(\text{PO}_4)_4$. A comparison of these values with those in Fig. 3 of this reference indicates the possibility of the three magnon-mediated exchange enhanced relaxation process is less probable in this compound, compared to that of the Raman process. The up-

per inset of Fig. 5 shows that the variation in $1/T_1$ with T follows the relation $1/T_1 \propto [(T-T_N)/T_N]^{-\alpha}$ in the range $16 \text{ K} < T < 50 \text{ K}$, with $T_N=16 \text{ K}$ and $\alpha=0.5$. The value of α is in close agreement with the theoretical prediction for a three-dimensional Heisenberg antiferromagnet.¹⁶

IV. CONCLUSION

We have investigated the static and the dynamic magnetic properties of the trimer spin chain compound $\text{Ca}_3\text{CuNi}_2(\text{PO}_4)_4$ (which is known to undergo an AF ordering near 20 K), using ^{31}P NMR studies in presence of the external magnetic fields of 1.39 and 7.04 T, in the temperature range 4–300 K. At any temperature, in the range 16–300 K, the spectrum corresponds to a typical overlap of two powder patterns, consistent with two inequivalent phosphorous sites, having different component of shift parameters. The NMR results also suggest an enhancement of interchain exchange interaction in $\text{Ca}_3\text{CuNi}_2(\text{PO}_4)_4$ compared to that in $\text{Ca}_3\text{Cu}_3(\text{PO}_4)_4$ ($T_C=0.91 \text{ K}$), which could be a reason for the

enhanced T_N in the former. The NMR line shape below T_N shows the signature of a considerable distribution of the internal magnetic field in the ordered state with the existence of two magnetic sublattices with opposite direction of polarization with respect to the direction of the external magnetic field. Behavior of $1/T_1$ in the temperature range 26–300 K shows the typical feature of fast spin fluctuation ($\omega_e \gg \omega_n$) of the paramagnetic moments. However, a comparison of the magnitude of $1/T_1$ with that of the calculated one indicates some additional fluctuating field possibly from orbital motion of the $3d$ electrons apart from spin also contribute to the relaxation process in the temperature region. Variation in ($1/T_1$) with T shows a clear signature of the appearance of long-range magnetic order in $\text{Ca}_3\text{CuNi}_2(\text{PO}_4)_4$ below 16 K (T_N). A comparison of the behavior of the $1/T_1$ data in $\text{Ca}_3\text{CuNi}_2(\text{PO}_4)_4$ with those in $\text{Sr}_3\text{Cu}_3(\text{PO}_4)_4$ clearly suggests that the mechanism of the relaxation changes from a two magnon-mediated Raman process in the former to a three magnon-mediated process in the latter.

*kajal.ghoshray@saha.ac.in

- ¹P. Lemmens, G. Güntherodt, and C. Gros, *Phys. Rep.* **375**, 1 (2003).
- ²F. D. M. Haldane, *Phys. Rev. Lett.* **50**, 1153 (1983).
- ³J. C. Bonner, S. A. Friedberg, H. Kobayashi, D. L. Meier, and H. W. J. Blöte, *Phys. Rev. B* **27**, 248 (1983).
- ⁴K. Hida, *J. Phys. Soc. Jpn.* **63**, 2359 (1994).
- ⁵M. Azuma, T. Odaka, M. Takano, D. A. Vander Griend, K. R. Poeppelmeier, Y. Narumi, K. Kindo, Y. Mizuno, and S. Maekawa, *Phys. Rev. B* **62**, R3588 (2000).
- ⁶M. Drillon, M. Belaiche, P. Legoll, J. Aride, A. Boukhari, and A. Moqine, *J. Magn. Magn. Mater.* **128**, 83 (1993).
- ⁷A. A. Belik, A. Matsuo, M. Azuma, K. Kindo, and M. Takano, *J. Solid State Chem.* **178**, 709 (2005).
- ⁸A. Podlesnyak, V. Pomjakushin, E. Pomjakushina, K. Conder,

and A. Furrer, *Phys. Rev. B* **76**, 064420 (2007).

- ⁹V. Yu. Pomjakushin, A. Furrer, D. V. Sheptyakov, E. V. Pomjakushina, and K. Conder, *Phys. Rev. B* **76**, 174433 (2007).
- ¹⁰B. J. Mean, K. H. Kang, J. H. Kim, I. N. Hyun, M. Lee, and B. K. Cho, *Physica B* **378-380**, 600 (2006).
- ¹¹S. Yamamoto, H. Hori, Y. Furukawa, Y. Nishisaka, Y. Sumida, K. Yamada, K. Kumagai, T. Asano, and Y. Inagaki, *J. Phys. Soc. Jpn.* **75**, 074703 (2006).
- ¹²M. Ghosh, K. Ghoshray, B. Pahari, R. Sarkar, and A. Ghoshray, *J. Phys. Chem. Solids* **68**, 2183 (2007).
- ¹³T. Moriya, *Prog. Theor. Phys.* **16**, 23 (1956).
- ¹⁴S. Giri, H. Nakamura, and T. Kohara, *Phys. Rev. B* **72**, 132404 (2005).
- ¹⁵H. Hori and S. Yamamoto, *J. Phys. Soc. Jpn.* **73**, 1453 (2004).
- ¹⁶T. Moriya, *Prog. Theor. Phys.* **28**, 371 (1962).